

REINFORCED CONCRETE IN TENSION: THE IMPORTANCE OF MODELLING TENSION STIFFENING

W.G.Kingston¹, P. Pankaj¹, A.S. Usmani¹, J.L. Torero¹

¹BRE Centre for Fire Safety Engineering, School of Engineering, The University of Edinburgh, Edinburgh, UK
E-mail of corresponding author: pankaj@ed.ac.uk

ABSTRACT

Tensile behaviour of concrete is often overlooked as it is assumed, by many design codes, to have limited impact on overall structural design. However, inclusion of appropriate tensile properties is essential in many situations to achieve realistic numerical models. This is particularly important in tanks and containment vessels where tensile stresses are likely to occur and could potentially lead to functional failure. It is widely accepted that plain concrete fails in tension through localised cracking and the post-peak softening behaviour can be defined in numerical models using energy based data or mesh adjusted strain values to ensure mesh insensitivity in finite element simulation. If reinforcement is introduced to a concrete section, tension stiffening occurs in the uncracked regions of concrete in addition to strain softening. The existence of tension stiffening is now recognised in literature and also by some design standards. The presence of tension stiffening implies that the behaviour of reinforced concrete cannot be simulated by simply including the constitutive models for reinforcement and concrete discretely. While strain softening is due to strain localisation, tension stiffening is a distributed phenomenon. This raises the question of how material properties in numerical models should be applied and adjusted according to element sizes in a finite element model. In the recent round robin analysis for the ultimate load capacity assessment of BARC containment (BARCOM) test model tension stiffening was ignored by most participants. Novel benchmark tests are developed and used to show that modelling based only on fracture energy for concrete and perfect von Mises plasticity for reinforcement leads to mesh sensitivity for reinforced concrete sections. Methods to incorporate tension stiffening are discussed and their efficacy examined using the developed benchmark tests.

INTRODUCTION

The issue of mesh sensitivity when modelling concrete numerically is well recognised and is a result of progressive failure through localised cracking. In plain concrete, loaded in tension, the post peak softening behaviour can be modelled using energy based properties which eliminate the dependence of results on element dimensions and therefore avoid mesh sensitivity. When reinforcement is introduced the situation becomes more complex as the post peak behaviour results from the combined effects of tension softening and tension stiffening. While strain softening is a result of strain localisation in cracked regions, stiffening is described as a macroscopic property which can be applied over a large area [1]. The presence of the additional tension stiffening effect suggests that reinforced concrete cannot be accurately modelled simply by applying constitutive models for steel and concrete discretely. It has been suggested [2] that tension stiffening has a more significant impact on overall behaviour when a low reinforcement ratio (ρ) is used and a ratio above 3% is cited as showing little mesh sensitivity.

Most of the concrete used in construction includes reinforcement, in some cases with ratios of below 3%, so a reliable constitutive model for reinforced concrete is essential if realistic numerical models are to be produced. Models that use standard steel properties along with modified concrete curves to incorporate tension stiffening have been proposed by a number of authors [3-7]. Figure 1 shows a comparison of the concrete curves obtained from three of these models [3, 4, 7], none of which use fracture energy. In all cases, the gradient of the pre-cracking branch is determined by the elastic modulus, E , up to a cracking stress, f_{ct} , but beyond this point they show a degree of variation in their shapes. The CEB Cracking Manual [7] begins by defining reinforced concrete behaviour and then identifies the contribution of concrete as the difference between this curve and that of bare steel with an area equal to the reinforcement. Stramandinoli and La Rovere [3] cite the CEB Cracking Manual's approach as a starting point but ultimately produce an exponential formula based on the reinforcement ratio, ρ , and steel-concrete modular ratio, n . It can be seen in Fig. 1 that both approaches produce very similar post peak curves. Gupta and Maestrini [4] present a series of formulae to determine various points leading to a trilinear post-cracking curve, which varies significantly from the previous two. It can be noted that, while the shapes of the graphs vary, they all reach zero at the same strain value ($\epsilon_{ct,0}$), regardless of element size. This is based on the assumption that total section loading cannot rise above the capacity of the steel reinforcement as it will have to carry all of the loading in the fully cracked

regions. The strain value at which concrete reaches zero is therefore the value at which steel yield stress is reached ($\epsilon_{ct,0} = \epsilon_y$).

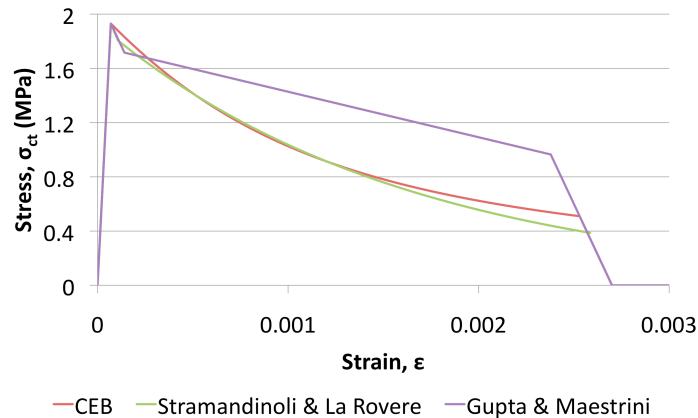


Figure 1: Constitutive concrete models proposed by various authors [7, 3, 4]

Cervenka and Purkl [5] and Feenstra and De Borst [6] identify a strain based tension stiffening graph which can be combined with the softening curve to obtain the combined effect of both phenomena and these are shown in Fig. 2. As with the previous models pre-cracking behaviour, up to cracking stress, f_{ct} , is defined by the elastic modulus, E , but the post-cracking region of the softening curve is defined using fracture energy. The stress value for the stiffening curve increases from the point at which cracking begins ($\epsilon_{ct,cr}$) until the softening curve reaches zero stress ($\epsilon_{ct,0}$, this value changes on the basis of element size), ultimately reaching a plateau which is defined as a proportion ($0 < \alpha < 1$) of the cracking stress. Similar to the previous models, the final branch of the stiffening curve is determined by reinforcement properties to ensure that total section load does not increase beyond that which could be carried by bare steel. This approach of starting out with an energy based curve for the softening behaviour and a separate curve for stiffening is significant as concrete properties are thought to have a much larger influence in the earlier stages of post-crack loading while later behaviour is determined largely by the steel reinforcement. The proposed model would allow scaling for different element sizes in the region immediately after cracking when concrete behaviour is believed to be most important.

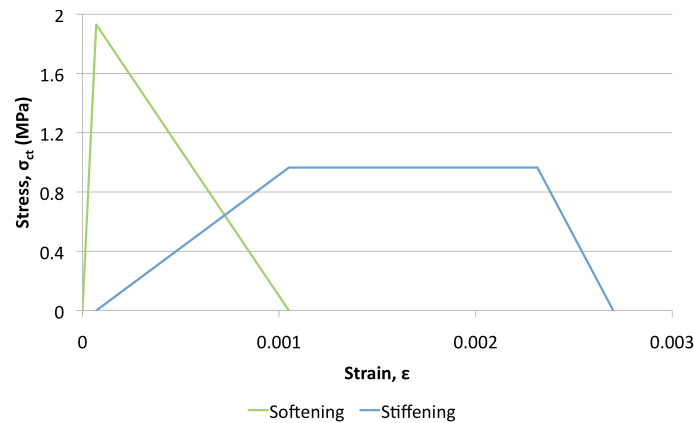


Figure 2: Softening and stiffening curves for constitutive concrete model proposed by Cervenka and Pukl [5] and Feenstra and de Borst [6]

PROPOSED BENCHMARK TEST

Figure 3 shows a novel model developed to conduct benchmark tests to investigate the significance of tension stiffening and mesh sensitivity. Three different meshes were considered (1x1, 3x3, 5x5) and section

thickness was varied in each column of the multi element models but the same material properties have been retained throughout. If a uniaxial displacement controlled load (δ) was applied to a multi element model with uniform section thickness, a homogenous stress distribution would arise and all of the elements would reach the cracking stress at the same time. The variable thickness was introduced to induce localised cracking in the thinnest region of each model where the uniform section load would cause a stress concentration. In each case the central column was assigned a thickness of 1mm with a variation between steps of 0.05mm. This approach maintained the same average thickness (1mm) in each model and this value was used to calculate the reinforcement ratio.

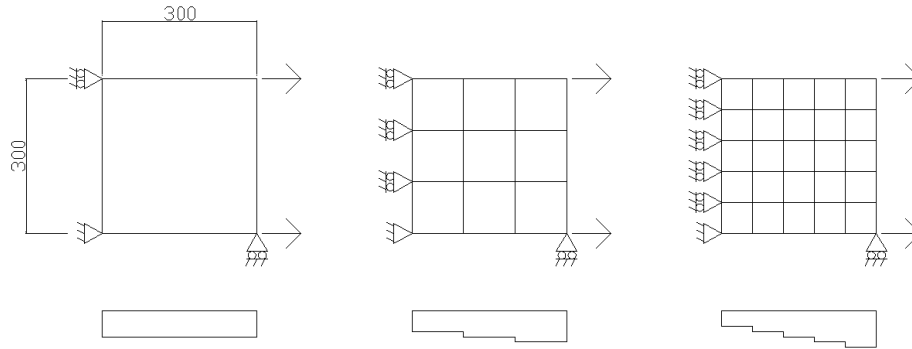


Figure 3: Proposed model showing three different meshes (dimensions in mm)

The models were developed using Abaqus finite element software with post peak behaviour specified using concrete damaged plasticity. Plane stress shell elements were used for the concrete and a perfect bond with the reinforcing bars was assumed. Although a perfect bond does not allow for the effects of bond slip it was considered to be an appropriate approximation as it is commonly used in analyses of real structures.

Models Using Plain Concrete

Initially, plain models were analysed to confirm that stress localisation, leading to cracking, occurred in the thinnest region of each model. Post peak behaviour was defined using fracture energy and the material properties are listed in Table 1 and the results are shown in Fig. 4.

Table 1: Concrete input properties for plain models

Elastic modulus, E (MPa)	27580
Cracking stress, f_{ct} (MPa)	1.93
Fracture energy, G_f (N/mm)	0.1
Poisson ratio, ν	0.2

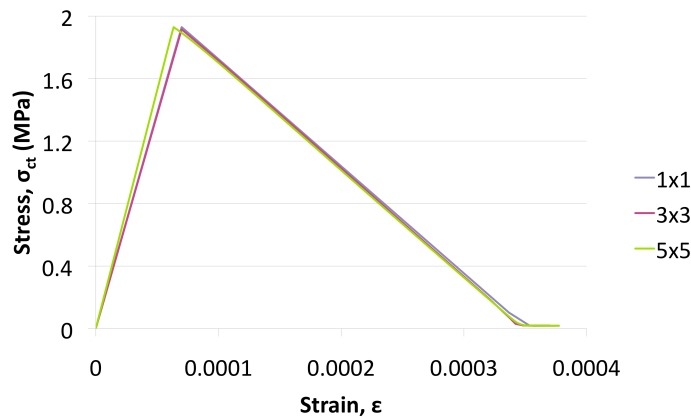


Figure 4: Pre and post-cracking behaviour for plain concrete ($\epsilon=\delta/l$)

As expected cracking was only observed in the thinnest part of each model and, following crack initiation, the thicker regions began to unload eventually reaching zero stress. The results confirm that the use of fracture energy in plain models leads to mesh insensitivity. The slight variation in gradients for the elastic phase of each model can be explained by the varying section thickness as the stress values were calculated from the total end load for each model.

Models Using Discrete Material Properties

To identify the impact of modelling concrete and reinforcement discretely, steel rebar was introduced to the plain models without altering the concrete properties. The reinforcing steel was given an elastic modulus, $E_c = 200000\text{MPa}$ and yield stress, $\sigma_y = 540\text{MPa}$. Two different reinforcement ratios were tested and the results can be seen in Figs. 5 & 6 where stress has been calculated as steel stress in a fully cracked region ($\sigma=N/A_s$) for a given end load, N and average strain ($\epsilon=\delta/l$) has been calculated from the applied displacement and section width, l . The point at which each reinforced concrete curve meets the bare steel curve in both figures represents the point at which concrete stress in at least one region has reached zero and section loading will therefore be entirely dependent on steel properties. It can be seen in Fig. 5 that, when $\rho=1.25\%$, there is significant mesh sensitivity with stress quickly falling to that of bare steel in the 1x1 mesh but rising at varying rates in the multi element models despite the use of fracture energy for concrete. The drop in stress in the 1x1 model is a result of the steep gradient of the post-cracking concrete curve for this element size, which outstrips the rate of increase in the reinforcement load.

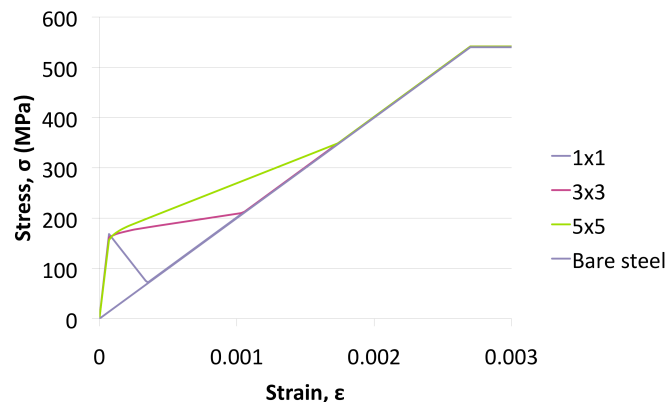


Figure 5: Reinforced concrete behaviour ($\sigma=N/A_s$, $\epsilon=\delta/l$) with concrete defined using fracture energy and $\rho=1.25\%$

When the reinforcement ratio is increased to $\rho=3.75\%$ (Fig. 6) mesh sensitivity reduces substantially because the increased quantity of reinforcement accounts for a larger proportion of total section load and therefore has a much more significant impact on its behaviour. It can be observed in Fig. 6 that stress rises continuously in all meshes although the rate of this increase and the point at which concrete stress reaches zero still varies.

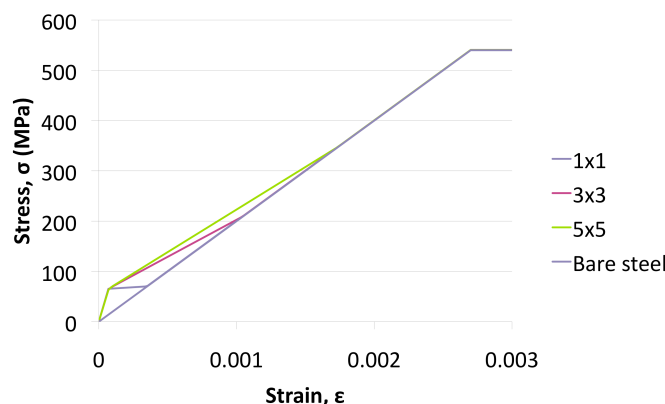


Figure 6: Reinforced concrete behaviour ($\sigma=N/A_s$, $\epsilon=\delta/l$) with concrete defined using fracture energy and $\rho=3.75\%$

By comparing Figs. 5&6 it is clear that the results for the lower reinforcement ratio show greater mesh sensitivity during the period of loading immediately after cracking although ultimate failure is controlled by the reinforcement in all cases as concrete stress has reached zero. The mesh sensitivity in Figs 5&6 can be explained by comparing the concrete models in Fig. 1 with energy based input properties. All of the models in Fig. 1 reach zero stress at $\epsilon=\epsilon_y$, regardless of element size, but because fracture energy is based on a stress-cracking displacement graph the maximum concrete strain, $\epsilon_{ct,0}$, will vary with mesh density.

To investigate the failure sequence within the finest mesh concrete stresses (Fig. 7) were studied. As would be expected, stress values were consistent throughout each column, with the first cracks occurring in the thinnest region. In contrast to the plain models, where cracking in a single region was followed by unloading in the others, multiple cracks occurred in the reinforced model as the presence of steel allowed the section load to continue increasing after crack initiation. The columns cracked in order of thickness, from thinnest to thickest, leading to the kind of distributed crack pattern that would be expected in reinforced concrete. It can be noted that once concrete stress reached zero ($\epsilon=0.0017$), behaviour throughout the model became reasonably uniform until steel yield ($\epsilon_y=0.0027$) occurred. As concrete stress had already reached zero much earlier in the loading sequence (Fig. 7) the section load would have been entirely dependent on the reinforcement so steel yield occurred in all five columns once yield strain, ϵ_y , was reached.

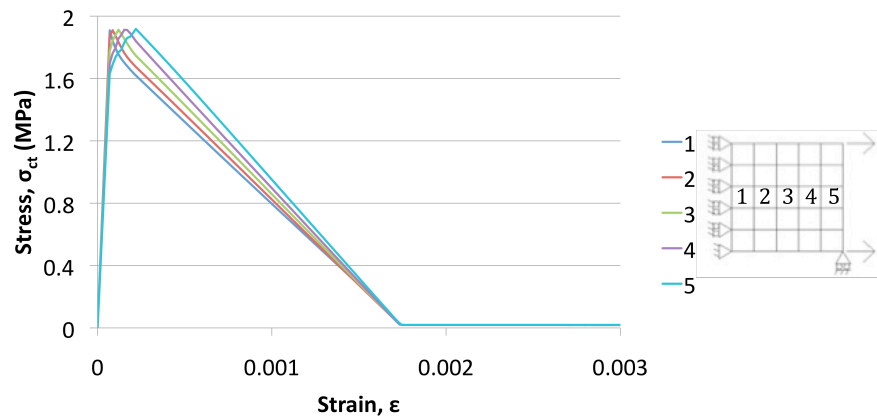


Figure 7: Concrete stress against average strain ($\epsilon=\delta/l$) with concrete defined using fracture energy and $\rho=1.25\%$

Incorporating tension stiffening

The above results show that, in some cases at least, reinforced concrete models based on discrete material properties lead to a significant degree of mesh sensitivity in the results. To assess the impact of incorporating tension stiffening the benchmark tests discussed previously were rerun with the concrete properties adjusted to take the form shown in Fig. 8. These graphs have been created by combining softening and stiffening curves of the form shown in Fig. 2. This constitutive model is derived partly from concrete fracture energy but is also influenced by steel properties. To maintain consistency the same fracture energy ($G_f=0.1N/mm$) was retained.

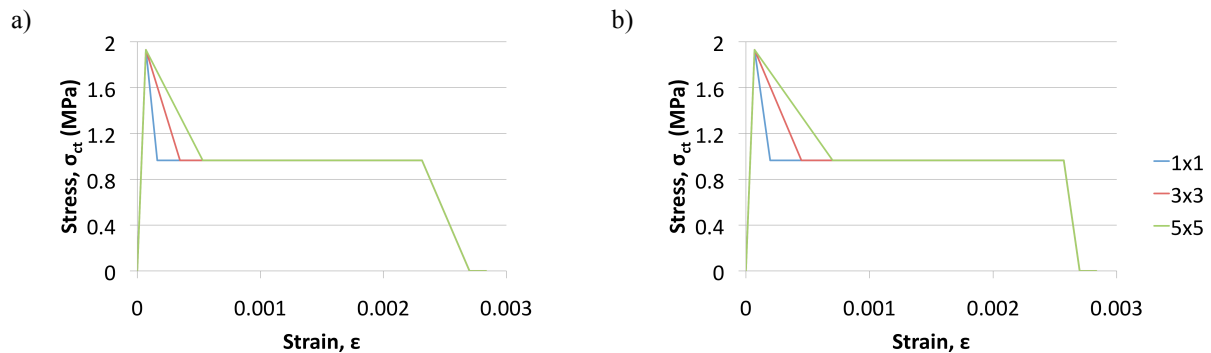


Figure 8: Concrete input properties for different meshes with a) $\rho=1.25\%$ and b) $\rho=3.75\%$

Steel stress in fully cracked regions, calculated from the total end load, N , can be observed in Figs. 9&10. As would be expected the maximum stress value obtained was 540MPa, which is equal to the steel yield stress, in all cases. It can also be observed that with a low reinforcement ratio there is much better agreement between different meshes when using the current concrete model than there was when discrete properties were applied. Some mesh sensitivity can still be observed in the earlier stages of loading, when the concrete will have a much bigger impact on load carrying ability. Sequential cracking was observed in all models with the first cracks forming in the thinnest regions and other regions cracking in order of thickness. In Fig. 9 the individual cracking of each column can be identified for the 3x3 mesh as well as the onset of cracking in the 1x1 model. As the region of the concrete input curve shows a steep drop immediately after cracking, section stress drops briefly before beginning to rise again. This is not visible in Fig. 10 as the load carrying capacity of concrete is less influential because of the increased steel ratio. Agreement between meshes improves in the later stages as concrete's contribution to overall section strength becomes less significant. This is more in keeping with expected behaviour for reinforced concrete than the discrete models discussed previously where stiffening was ignored. Although some mesh sensitivity is evident immediately after cracking in both figures the general behaviour of all of the models is relatively similar.

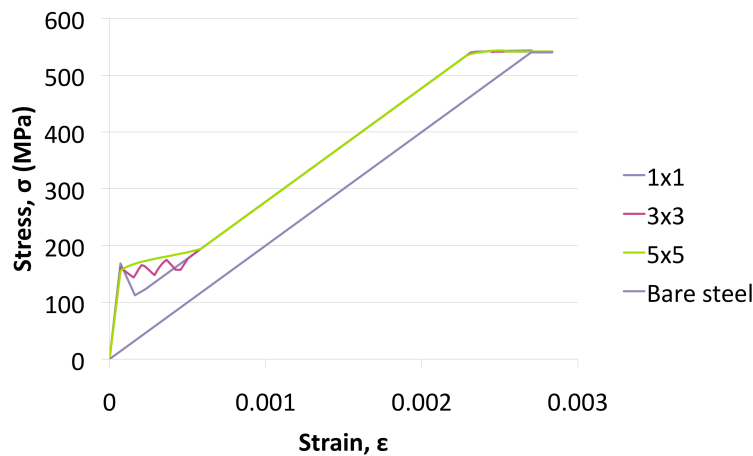


Figure 9: Reinforced concrete behaviour ($\sigma=N/A_s$, $\epsilon=\delta/l$) with concrete defined using curves in Fig. 9a and $\rho=1.25\%$

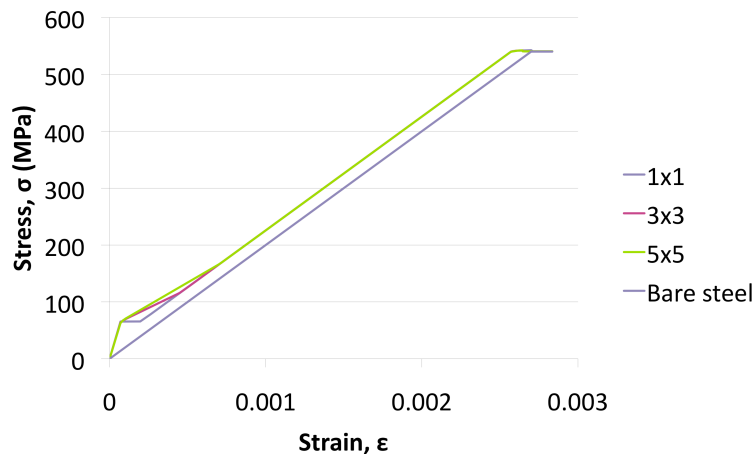


Figure 10: Reinforced concrete behaviour ($\sigma=N/A_s$, $\epsilon=\delta/l$) with concrete defined using curves in Fig. 9b and $\rho=3.75\%$

Element Dimensions Ignored

In the models incorporating tension stiffening the main area of mesh sensitivity appeared to coincide with the region of the concrete curve that was adjusted according to element size. The decision was therefore taken to rerun analyses for all three meshes using the properties for a 3x3 mesh from Fig. 8 and the results are shown in Fig. 11. Mesh sensitivity appears to have been significantly reduced by making this adjustment to the concrete properties and the failure sequence is clearly visible for all three meshes. As before, concrete regions cracked sequentially from thinnest to thickest and the general behaviour is quite similar to that shown in the mesh adjusted models.

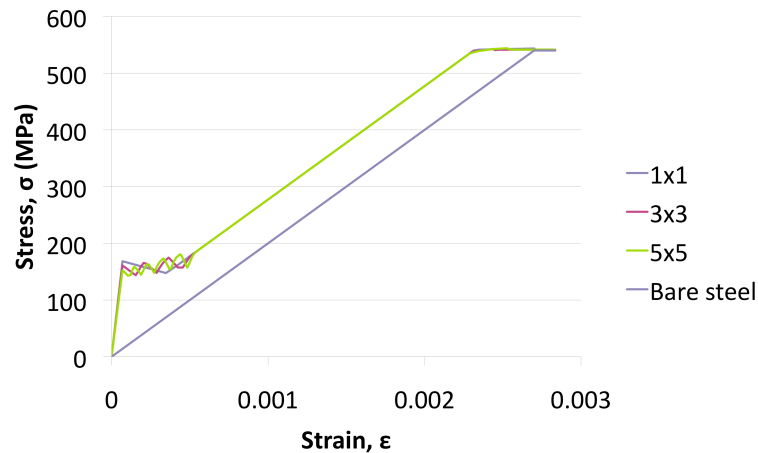


Figure 11: Reinforced concrete behaviour ($\sigma=N/A_s$, $\epsilon=\delta/l$) with concrete defined using 3x3 curve in Fig. 9a and $\rho=1.25\%$

CONCLUSIONS

The results certainly suggest that it is important to incorporate tension stiffening into numerical reinforced concrete models particularly for situations where a low reinforcement ratio is to be used. Results from models incorporating tension stiffening but ignoring element size suggest that stiffening behaviour is the much more important feature in preventing mesh sensitivity. This is encouraging as it seems to justify the use of concrete curves, such as those shown in Fig. 1, which cannot easily be adjusted according to mesh density but do incorporate both softening and stiffening behaviour.

ACKNOWLEDGEMENTS

The first author gratefully acknowledges funding from the BRE Trust and support from Dr Debbie Smith.

REFERENCES

1. Bentz, E. et al., "Essential nonlinear modelling concepts", Practitioners' guide to finite element modelling of reinforced concrete structures, pp. 83-119, June, 2008.
2. Koeberl, B., and Willam, K., "Question of tension softening versus tension stiffening in plain and reinforced concrete", Journal of Engineering Mechanics, Vol. 134, No. 9, 2008, pp. 804-808
3. Stramandinoli, R., And La Rovere, H., "An efficient tension-stiffening model for nonlinear analysis of reinforced concrete members", Engineering Structures, Vol. 30, 2008, pp. 2069-2080
4. Gupta, A., and Maestrini, S., "Tension stiffness model for reinforced concrete bars", Journal of Structural Engineering, Vol. 116, No. 3, 1990, pp. 769-790
5. Cervenka, V., and Pukl, R., "Computer simulation of anchoring technique in reinforced concrete beams", Computer Aided Analysis and design of concrete structures, N. Bicanic et al., Pineridge Press, Swansea, UK, 1990, pp. 1-21

6. Feenstra, P., and de Borst, R., "Constitutive model for reinforced concrete", *Journal of Engineering Mechanics*, Vol. 121, No. 5, 1995, pp. 587-595
7. Comité Euro-International du Béton, "Cracking and deformations", A, Beeby et al., *École Polytechnique Fédérale De Lausanne*, Switzerland, 1985